Trees (2014) 28:1859–1865
DOI 10.1007/s00468-014-1063-5

SHORT COMMUNICATION

# Automatic measurement of stomatal density from microphotographs

**Silvère Vialet-Chabrand · Oliver Brendel**

Received: 10 January 2014 / Revised: 18 July 2014 / Accepted: 28 July 2014 / Published online: 31 August 2014


**Abstract**
***Key message*** **An automated process using a cascade classifier allowed the rapid assessment of the density and distribution of stomata on microphotographs from leaves of two oak species.**
*Abstract* Stomatal density is the number of stomata per unit area, an intensively studied trait, involved in the control of $CO_2$ and $H_2O$ exchange between leaf and atmosphere. This trait is usually estimated by counting manually each stoma on a given surface (e.g., a microphotograph), usually repeating the procedure with images from different parts of the leaf. To improve this procedure, we tested the performance of a cascade classifier to automatically detect stomata on microphotographs from two oak species: *Quercus afares* Pomel and *Quercus suber* L. The two species are phylogenetically close with similar stomatal morphology, which allowed testing the reuse of the cascade classifier on stomata with similar shape. The results showed that a cascade classifier trained on only 100 sample views of stomata from *Q. afares* was able to rapidly detect stomata in *Q. afares* as well as in *Q. suber* with a very low number of false positives (5 %/1.9 %) and a small number of undetected stomata (14.8 %/0.74 %), when partial stomata near the edge of the microphotographs were ignored. The remaining undetected stomata were due to obstacles such as trichomes. As an example of further applications, we used the positions detected by the cascade classifier to assess the spatial distribution of stomata and group them on the leaf surface. To our knowledge this is the first time that a cascade classifier has been applied to plant microphotographs, and we were able to show that it can dramatically decrease the time needed to estimate stomatal density and spatial distribution.

**Keywords** Stomatal density · Stomatal distribution · Leaf anatomy · Object detection · Cascade classifier

## Introduction

The control of gas exchange from leaf to air is estimated by measuring stomatal conductance, a trait that primarily depends on the aperture of the stomatal pore and the number of stomata (Franks and Farquhar 2001). Stomatal morphology, spatial distribution, and behaviour respond to a spectrum of signals, from intracellular signalling to global climatic change, and are often estimated by studying stomatal size and density (Hetherington and Woodward 2003; Assouline and Or 2013). Stomatal density is defined as the number of stomata per unit area and displays a large intra and inter-specific diversity (Woodward and Kelly 1995; Delgado et al. 2011).

The estimation of stomatal density usually requires a microphotograph or an imprint of the leaf surface (Hultine and Marshall 2001), by using optical microscopy or scanning electron microscopy (SEM). The microphotograph is used to count each stoma manually on a small part of the

Communicated by L. Gratani.

S. Vialet-Chabrand (✉) · O. Brendel
INRA, UMR1137 "Ecologie et Ecophysiologie Forestières",
542802 Champenoux, France
e-mail: silvere@vialet-chabrand.com

O. Brendel
e-mail: brendel@nancy.inra.fr

S. Vialet-Chabrand · O. Brendel
Faculté des Sciences, Université de Lorraine,
UMR1137 "Ecologie et Ecophysiologie Forestières",
54500 Vandoeuvre, France

leaf surface (Akita et al. 2013). The procedure is repeated from different parts of a leaf to compensate for the non-uniform stomatal distribution (Roussel et al. 2009). The manual counting of stomata on several microphotographs is very time consuming and could be improved by automatizing the detection of stomata.

A process that automatically and rapidly detects stomata on a microphotograph with a small number of false positives would be very useful in estimating stomatal density and spatial distribution when a large number of leaves need to be processed, e.g., for analyses of genetic diversity (Brendel et al. 2008). Black and white microphotographs obtained from SEM limit the number of algorithms that are able to detect stomata without colour. Depending on the species observed, stomata might not be clearly delimited due to the presence of wax, which prohibits using differences in brightness as proposed by Salomon et al. (2010). Viola and Jones (2001) described a machine learning approach for visual object detection, which is capable of processing images rapidly and achieving high detection rates. This approach was named cascade classifier and was improved by Lienhart and Maydt (2002). The objective of this research was to test the performance of the cascade classifier for rapid detection of stomata using SEM microphotographs of *Quercus afares* Pomel leaves. We also tested if the use of the cascade classifier trained for *Q. afares* could be extended, by applying it to leaves of phylogenetically close species, *Quercus suber* L. Moreover, the automatic detection of stomata not only yields the number of stomata within an image, but also their precise position. Therefore, we propose as an example of the usage of this data the analysis of the heterogeneity of stomatal density within an image.

## Materials and methods

### Plant material

Three discs (1 $cm^2$) were punched from different areas of each leaf. They were immediately frozen in liquid nitrogen and stored at −80 °C. Microphotographs were made with a variable pressure scanning electron microscope (model 1450VP, Leo, Cambridge, UK, 20–60 Pa inside chamber, accelerating voltage 15 kV, working distance 13 mm). Microphotographs at 300× of the abaxial epidermis (0.503 $mm^2$) were taken for each disc to estimate stomatal density and test the cascade classifier.

### Implementation of the cascade classifier

The cascade classifier used was a part of an open source library for computer vision and machine learning software: OpenCV (http://www.opencv.org). OpenCV is freely available and supports many programming languages. Consequently, the application developed here could be easily shared and integrated into other softwares. We used the functions provided by the OpenCV library to implement a small command line program in C++ that detects the number of stomata. Additionally, undetected stomata and false positives can be corrected visually on microphotographs.

### Haar feature-based cascade classifier

The cascade classifier consists of a succession of several simpler classifiers (stages) that are trained using boosting techniques based on two collections of images that contain or not contain the object of interest (here, stomata). The cascade classifier works with haar-like features (basically the difference between the sum of image pixels in two defined areas), which are more synthetic and informative than only pixel values. After training, the cascade classifier can be applied to a region of an image contained in a detection window, until at some stage the candidate region is rejected (classified as non-stomata) or all the stages are passed. The cascade classifier outputs a "1" if the region is likely to show the object of interest and "0" otherwise. To search for the object of interest in the whole image, the detection window can be moved across the image to check every location using the classifier. The classifier is designed so that it can scale the detection window to find the objects of interest at different sizes, which is more efficient than resizing the image itself.

### Data preparation

To train the cascade classifier, one hundred sample views of stomata were cropped manually from several microphotographs of *Q. afares* leaves (Fig. 1). From each original sample view, 100 views were generated using the command line tools provided by the OpenCV library that applied distortions (random rotation around all three axes, colour threshold; see "Appendix Data preparation"). This resulted in 10,000 sample views of stomata scaled to the same size (9 × 9 pixels). For each original sample view, a binary file was generated that contained the transformed sample views. All binary files were merged into one unique file that represents the collection of positive images using the mergevec command line tool (See "Appendix Data preparation"; source code: http://note.sonots.com/SciSoftware/haartraining.html). This collection of images was associated with a collection of 3,000 negative images that do not contain stomata to train the cascade classifier (provided by: http://tutorial-haartraining.googlecode.com/svn/trunk/data/negatives/).

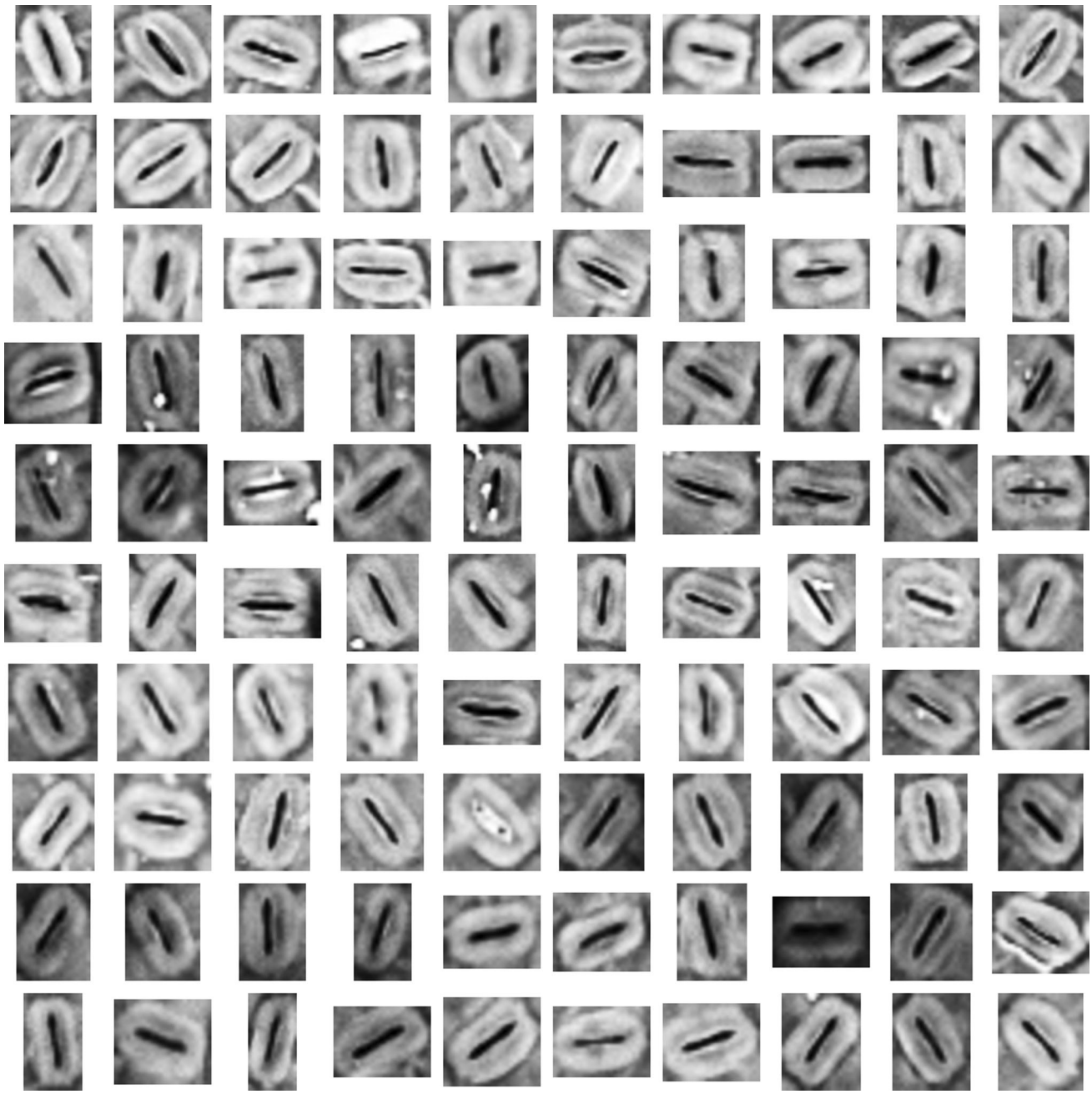

**Fig. 1** Sample views of stomata cropped from microphotograph and used to train the cascade classifier

## Training

The two collections of images were used to train the cascade classifier (http://docs.opencv.org/doc/user_guide/ug_traincascade.html). For each stage of the cascade classifier, simple classifiers were trained using one haar-like feature calculated on positive and negative examples until it reached the detection rate and the false alarm rate defined by the user (see "Appendix Training"). On a standard office computer (Core2Duo 2.5Ghz, 4Go RAM) this step can take a long time (up to several days) depending on the parameters specified by the user and the activation of multi-threading options in OpenCV. The training results in an xml file containing parameters of the cascade classifier which is used to detect stomata.

## Detection

The detection window is moved and scaled over the whole image to detect stomata of different size by using the

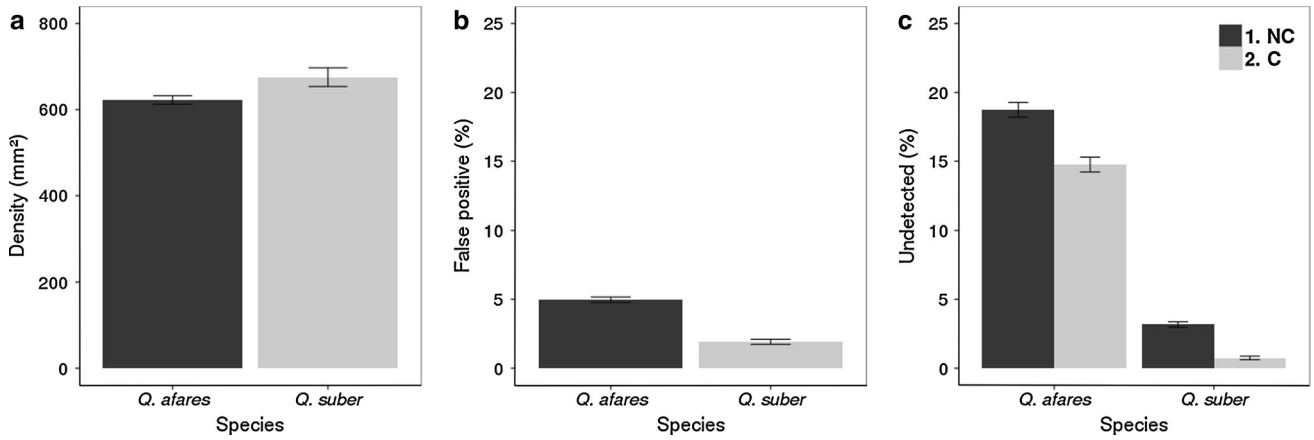


**Fig. 2** Stomatal density estimated from leaves of *Q. afares* ($n = 100$) and *Q. suber* ($n = 40$) (**a**) and performance of cascade classifier in estimating stomatal density on each species: percentage of false positives (object detected by error as stomata, **b**) and stomata not detected with (C) and without correction (NC) (**c**). *Error bars* represent mean ± standard error

detectMultiScale function provided by the OpenCV library (http://docs.opencv.org/modules/objdetect/doc/cascade_classification.html). Our program used this function and the file generated during training as an input, to detect the number of stomata and their position on the microphotographs. On a standard office computer (Core2Duo 2.5Ghz, 4Go RAM) this detection step takes less than 10 s.

### Detection performance

To test the performance of the cascade classifier, the number of false positives and of undetected stomata were estimated visually on microphotographs of different mature leaves from 1-year-old *Q. afares* (100 microphotographs) and *Q. suber* (40 microphotographs).

### Stomatal distribution

The stomatal distribution in the epidermis was investigated using the expectation maximization (EM) clustering algorithm included in the OpenCV library. In the EM function, we used the coordinates of stomata as inputs and the default parameters except for the number of groups for which we tested different values. We kept the number of groups that gave the best clustering. For each coordinate, the group and the likelihood of the prediction were calculated. The outliers (stomata included in a group, but not close to the centroid) with low likelihood were excluded by adjusting manually a threshold.

## Results

With the visual estimation, *Q. afares* and *Q. suber* displayed a mean stomatal density of 622 and 675 $mm^{-2}$, respectively

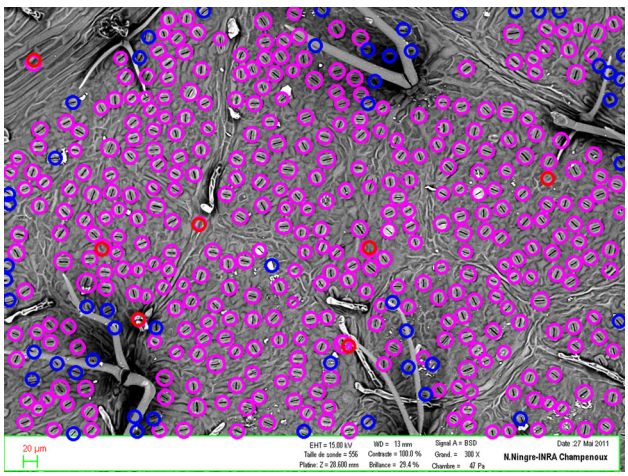


**Fig. 3** Stomatal detection using the cascade classifier for *Quercus afares*. *Circles* represent detected stomata (*pink*), undetected stomata (*blue*) and false positives (*red*) (colour figure online)

(Fig. 2a). A large number of stomata displayed by both species were successfully detected by the cascade classifier on all microphotographs, which was trained with only 100 original sample views of stomata of *Q. afares* (Fig. 3). On the microphotographs of *Q. afares* used to test the cascade classifier, the number of false positives was low and represented 5 ± 0.2 % (mean ± se) of the total number of stomata (Fig. 2b). Only some stomata were not detected representing 18.7 ± 0.5 % (mean ± se) of the total number of stomata (Fig. 2c). The undetected stomata were mainly localized on the border of the microphotograph and near trichomes, which resulted in an incomplete view of stomata and a large variation of brightness (Fig. 3). If the partial stomata near the edges were ignored, the rate of undetected stomata was 14.8 ± 0.5 % (Fig. 2c) in *Q. afares*.

The cascade classifier was also successfully applied on microphotographs from *Q. suber* with 1.9 ± 0.2 % of false positive (Fig. 2b) and 3.2 ± 0.2 % of undetected stomata (Fig. 2c). After correction for partial stomata, the rate of undetected stomata was 0.7 ± 0.1 % (Fig. 2c). The major difference between the two sets of images used to test the performance of the cascade classifier was the presence of a large number of trichomes on *Q. afares* microphotographs that have partially hidden stomata (Figs. 3, 4).

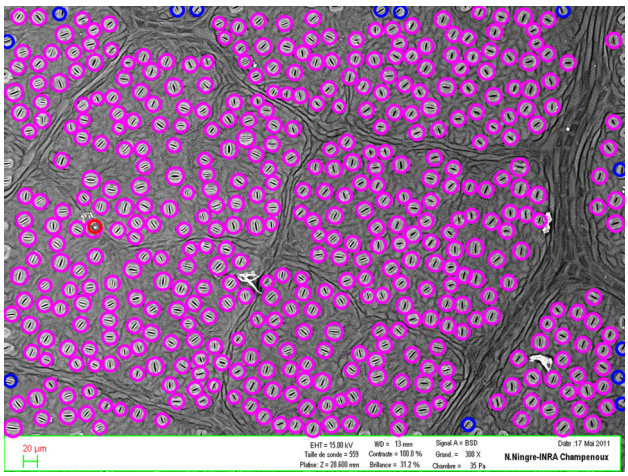


**Fig. 4** Stomatal detection using the cascade classifier for *Quercus suber*. *Circles* represent detected stomata (*pink*), undetected stomata (*blue*) and false positives (*red*) (colour figure online)

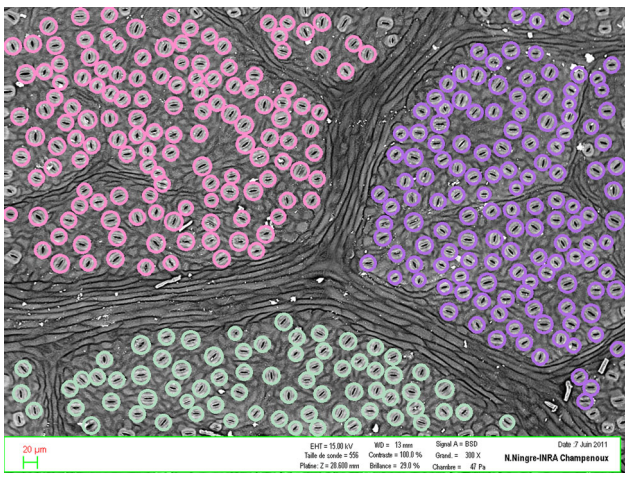


**Fig. 5** Stomatal distribution of detected stomata by cascade classifier in *Q. suber* and estimated by expectation maximization (EM) clustering (3 groups)

As can be seen in Fig. 5, the veinlets of a heterobaric leaf separated stomata into groups and formed a network of barriers. Coordinates of stomata obtained from the cascade classifier were used successfully to characterize the clustering of stomata with the EM algorithm, according to their distribution on the epidermis (Fig. 5).

## Discussion

Estimating stomatal density is often time consuming as it involves visually counting stomata on microphotographs (Hultine and Marshall 2001), or with the aid of an image processing software to assist the manual counting (Monclus et al. 2006; Tanaka and Shiraiwa 2009). Compared to these methods, our procedure using a cascade classifier has accurately and automatically detected stomata on microphotographs from different species. The performance varied depending on the presence or absence of trichomes which partially hid the stomata. With 85.2 % of detected stomata in *Q. afares*, this procedure reduces the time needed to count stomata and the remaining stomata can be counted visually. In *Q. suber*, the rates of false positives and undetected stomata were very low and therefore a visual correction was not needed. In these conditions, the cascade classifier could be used in a batch procedure.

By applying our procedure, it becomes easier to assess stomatal density in a large number of samples, which is necessary to study the diversity of this trait and investigate, as an example, the adaptive phenotypic plasticity in a changing climate (Nicotra et al. 2010). In this article, the similar morphology of stomata allowed using the cascade classifier on *Q. suber* even if it was trained on *Q. afares*. As the training of the cascade classifier is the time-consuming part of this approach, this opens the perspective to reuse the trained cascade classifier on species with similar stomatal morphology.

The automatic detection of stomata can be combined with other techniques to estimate further leaf traits and to open the way for a large range of applications. As an example, the spatial distribution of stomata can be studied with our procedure by using the stored position of the stomata. Zheng et al. (2013) had observed that this trait dramatically changed in response to experimental warming resulting in an increase of gas exchange with a potential impact on photosynthesis. Our procedure facilitates the measure of this parameter and could be used to investigate the effects of different distribution patterns on

gas exchange and adaptation to climate change. As a second example, Sellin et al. (2010) assessed the stomatal size manually on 1,000 stomata to investigate the relationship between the variation in stomatal conductance among trees and canopy layers. Our procedure could be extended to fit an ellipse on detected stomata and thus automatically estimate length and width of a large number of stomata with the advantage of the reproducibility of the method.

The cascade classifier is a very promising technique to detect objects on a large number of microphotographs and was successfully used for a fast estimation of stomatal density in two oak species. Further, our approach gives a quick access to other stomatal traits that could be used for plasticity and diversity studies.

**Author contribution** Silvère Vialet-Chabrand developed the methodology (programmes and scripts), analysed the results and prepared the manuscript. Oliver Brendel contributed to the development of the experimental setup and to manuscript writing.

**Acknowledgments** Silvère Vialet-Chabrand was supported by a doctoral grant from Université de Lorraine (France). The authors would like to thank the microscopy laboratory of the certified facility in Functional Ecology (PTEF OC 081) from UMR 1137 EEF and UR 1138 BEF at the research centre INRA Nancy-Lorraine, and in particular Didier Le Thiec and Nathalie Ningre for the sample preparation and treatment. The PTEF facility was supported by the French National Research Agency through the Laboratory of Excellence ARBRE (ANR-12-LABXARBRE-01), as well as by grants from FEDER, Région Lorraine and IFR 110. The UMR EEF 1137 was supported by the French National Research Agency through the Laboratory of Excellence ARBRE (ANR-12-LABXARBRE-01).

**Conflict of interest** The authors declare that they have no conflict of interest.

## Appendix

### Data preparation

The command line to apply distortions on each microphotograph was:

opencv_createsamples -img./Pos/img.tif -num 100 -bg bg.txt -vec samples.vec -maxxangle 0.5 -maxyangle 0.5 -maxzangle 6.7 -maxidev 10 -bgcolor 120 -bgthresh 0 -w 9 -h 9.

| Options | Values | Descriptions |
|---|---|---|
| -img | ./Pos/img.tif | A positive sample view |
| -num | 100 | The number of positive samples to be generated |
| -bg | bg.txt | Background description file; contains a list of images, which are used as a background for randomly distorted versions of the object |
| -vec | samples.vec | Name of the output file containing the positive samples for training |
| -maxxangle | 0.5 | The maximum rotation angle in *x*-direction in radians |
| -maxyangle | 0.5 | The maximum rotation angle in *y*-direction in radians |
| -maxzangle | 6.7 | The maximum rotation angle in *z*-direction in radians |
| -maxidev | 10 | The desired maximum intensity deviation of foreground samples' pixels |
| -bgcolor | 120 | The background colour considered as transparent |
| -bgthresh | 0 | All pixels within bgcolor±bgthresh are interpreted as transparent |
| -w | 9 | The resulting sample width |
| -h | 9 | The resulting sample height |

The command line to merge all binary files into one (merge.vec) used as input for a text file containing all filenames (samples.txt):

mergevec samples.txt merge.vec -w 9 -h 9.

| Options | Values | Descriptions |
|---|---|---|
| -w | 9 | The resulting sample width |
| -h | 9 | The resulting sample height |

### Training

The command line for training cascade classifier was:

opencv_traincascade -data./traininghaar -vec merge.vec -bg bg.txt -numPos 10,000 -numNeg 3,000 -numStages 18 -precalcValBufSize 500 -precalcIdxBufSize 500 -featuretype haar -w 9 -h 9 -minHitRate 1 -maxFalseAlarmRate 0.45 -mode BASIC -maxWeakCount 200 -weightTrimRate 0 -maxDepth 2

| Options | Values | Descriptions |
|---|---|---|
| -data | ./TrainingHAAR | The directory for the output files |
| -vec | merged.vec | Name of the input file containing the positive samples |
| -bg | bg.txt | Background description file; contains a list of images, which are used as a background for randomly distorted versions of the object |
| -numPos | 10,000 | Number of positive samples used in training for every classifier stage |
| -numNeg | 3,000 | Number of negative samples used in training for every classifier stage |
| -numStages | 18 | Number of cascade stages to be trained |
| -precalcValBufSize | 500 | Size of buffer for precalculated feature values (in Mb) |
| -precalcIdxBufSize | 500 | Size of buffer for precalculated feature indices (in Mb). The more memory you have, the faster is the training process |
| -featureType | HAAR | Type of features |
| -w | 9 | The resulting sample width |
| -h | 9 | The resulting sample height |
| -minHitRate | 1 | Minimal desired hit rate for each stage of the classifier. Overall hit rate may be estimated as (min_hit_rate^number_of_stages) |
| -maxFalseAlarmRate | 0.45 | Maximal desired false alarm rate for each stage of the classifier. Overall false alarm rate may be estimated as (max_false_alarm_rate^number_of_stages) |
| -mode | BASIC | Selects the type of haar feature set used in training. BASIC use only upright features |
| -maxWeakCount | 200 | Maximal count of weak trees for every cascade stage. The boosted classifier (stage) will have as many weak trees (≤maxWeakCount) as needed to achieve the given-maxFalseAlarmRate |
| -weightTrimRate | 0 | Specifies whether trimming should be used and its weight |
| -maxDepth | 2 | Maximal depth of a weak tree |

## References


Akita K, Hasezawa S, Higaki T (2013) Breaking of plant stomatal one-cell-spacing rule by sugar solution immersion. PLoS One 8:e72456. doi:10.1371/journal.pone.0072456

Assouline S, Or D (2013) Plant water use efficiency over geological time—evolution of leaf stomata configurations affecting plant gas exchange. PLoS One 8:e67757. doi:10.1371/journal.pone.0067757

Brendel O, Thiec D, Scotti-Saintagne C et al (2008) Quantitative trait loci controlling water use efficiency and related traits in *Quercus robur* L. Tree Genet Genomes 4:263–278. doi:10.1007/s11295-007-0107-z

Delgado D, Alonso-Blanco C, Fenoll C, Mena M (2011) Natural variation in stomatal abundance of *Arabidopsis thaliana* includes cryptic diversity for different developmental processes. Ann Bot 107:1247–1258. doi:10.1093/aob/mcr060

Franks PJ, Farquhar GD (2001) The effect of exogenous abscisic acid on stomatal development, stomatal mechanics, and leaf gas exchange in *Tradescantia virginiana*. Plant Physiol 125:935–942. doi:10.1104/pp.125.2.935

Hetherington AM, Woodward FI (2003) The role of stomata in sensing and driving environmental change. Nature 424:901–908. doi:10.1038/nature01843

Hultine KR, Marshall JD (2001) A comparison of three methods for determining the stomatal density of pine needles. J Exp Bot 52:369–373. doi:10.1093/jexbot/52.355.369

Lienhart R, Maydt J (2002) An extended set of Haar-like features for rapid object detection. Int Conf Image Process IEEE 1:900–903

Monclus R, Dreyer E, Villar M, Delmotte FM, Delay D, Petit JM, Brignolas F (2006) Impact of drought on productivity and water use efficiency in 29 genotypes of *Populus deltoides* × *Populus nigra*. New Phytol 169:765–777. doi:10.1111/j.1469-8137.2005.01630.x

Nicotra AB, Atkin OK, Bonser SP, Davidson AM, Finnegan EJ, Mathesius U, van Kleunen M (2010) Plant phenotypic plasticity in a changing climate. Trends Plant Sci 15:684–692. doi:10.1016/j.tplants.2010.09.008

Roussel M, Thiec D, Montpied P et al (2009) Diversity of water use efficiency among *Quercus robur* genotypes: contribution of related leaf traits. Ann For Sci 66:1–10. doi:10.1051/forest/2009010

Salomon S, Grunewald D, Stüber K et al (2010) High-throughput confocal imaging of intact live tissue enables quantification of membrane trafficking in *Arabidopsis*. Plant Physiol 154:1096–1104. doi:10.1104/pp.110.160325

Sellin A, Eensalu E, Niglas A (2010) Is distribution of hydraulic constraints within tree crowns reflected in photosynthetic water-use efficiency? An example of *Betula pendula*. Ecol Res 25:173–183. doi:10.1007/s11284-009-0641-2

Tanaka Y, Shiraiwa T (2009) Stem growth habit affects leaf morphology and gas exchange traits in soybean. Ann Bot 104:1293–1299. doi:10.1093/aob/mcp240

Viola P, Jones M (2001) Robust real-time object detection. Int J Comput Vis

Woodward FI, Kelly CK (1995) The influence of $CO_2$ concentration on stomatal density. New Phytol 131:311–327. doi:10.1111/j.1469-8137.1995.tb03067.x

Zheng Y, Xu M, Hou R, Shen R, Qiu S, Ouyang Z (2013) Effects of experimental warming on stomatal traits in leaves of maize (*Zea may* L.). Ecol Evol 3:3095–3111. doi:10.1002/ece3.674